Angiographic Classification of Tumor Attachment of Meningiomas at the Cerebellopontine Angle

Naoto Kunii[1], Takahiro Ota[1], Taichi Kin[1], Kyousuke Kamada[1], Akio Morita[2], Nobutaka Kawahara[3], Nobuhito Saito[1]

Key words
- Angiography
- Attachment
- Cerebellopontine angle
- Classification
- Meningioma

Abbreviations and Acronyms
CI: Confidence interval
CPA: Cerebellopontine angle
CTA: Computed tomography angiography
ICA: Internal carotid artery
MRA: Magnetic resonance angiography
MRI: Magnetic resonance imaging
WHO: World Health Organization

From the [1]Department of Neurosurgery, the University of Tokyo, Tokyo; [2]Department of Neurosurgery, Kanto Medical Center NTT EC, Tokyo; and [3]Department of Neurosurgery, Yokohama City University School of Medicine, Yokohama, Japan

To whom correspondence should be addressed: Nobuhito Saito, M.D., Ph.D. [E-mail: nsaito-tky@umin.net].

Citation: World Neurosurg. (2011) 75, 1:114-121.
DOI: 10.1016/j.wneu.2010.09.020

Journal homepage: www.WORLDNEUROSURGERY.org

Available online: www.sciencedirect.com

OBJECTIVE: **To present an angiographic classification of attachment of meningiomas at the cerebellopontine angle (CPA) based on tumor feeding and to validate the utility of this classification in predicting meningioma attachments at the CPA.**

METHODS: **The authors retrospectively analyzed 34 consecutive patients with meningioma at the CPA. Based on operative findings, tumors were classified into four types: the petroclival type, in which the trigeminal nerve is displaced laterally; the tentorial type, in which the center of tumor attachment is located at the medial tentorium; the anterior petrous type, in which the center of tumor attachment is located anterior to the meatus; and the posterior petrous type, in which the center of tumor attachment is located posterior to the meatus. Magnetic resonance imaging (MRI) was sufficient to confirm attachment of the posterior petrous type. Another 26 cases were analyzed angiographically and classified into three types: abnormal ipsilateral tentorial artery type (type A); bilateral internal carotid artery (ICA) type (type B); and nontentorial, non-ICA type (type N). This angiographic classification was validated by comparison with the attachment classification.**

RESULTS: **Angiographic types A, B, and N corresponded to tentorial, petroclival, and anterior petrous types of attachment. Observed agreement was very high, particularly for tumors greater than 30 mm in diameter (κ statistic 0.83; 95% confidence interval [CI] 0.62–1.0). Angiographic type in this paired attachment typing offered high sensitivity and specificity greater than 0.80 in tumors larger than 30 mm.**

CONCLUSIONS: **This angiographic classification seems to be useful in predicting meningioma attachments at the CPA. The existence of an abnormally developed tentorial artery seems highly indicative of tumor attachment to the tentorium.**

INTRODUCTION

Although advances in skull base techniques have dramatically decreased mortality and morbidity associated with resection of meningiomas at the cerebellopontine angle (CPA), surgery for this region remains challenging (2, 3, 11, 18, 25, 28). Other than advances in operative techniques, there are two major factors that are expected to promote further improvement in the operative outcome. One is preoperative knowledge of the consistency and the World Health Organization (WHO) grading of the lesion. In the last 2 decades, a high correlation has been shown between hyperintensity of meningioma on T2-weighted magnetic resonance imaging (MRI) and soft consistency of the tumor, which is sometimes associated with WHO high grade or high vascularity (4, 19, 29, 30, 33). Knowing these characteristics of the tumor could greatly influence extent of craniotomy, estimation of operative time, and risk-benefit assessment. The other factor is preoperative knowledge of tumor attachment, which is of greater importance than the former factor, especially in this difficult location, because knowledge of tumor attachment not only has a strong influence on the above-mentioned preoperative evaluations but also might change the operative approach itself.

To investigate surgical approaches in greater detail, numerous surgeons have proposed various attachment classifications for meningioma at the CPA (3, 16, 20, 26, 27, 32). Based on intraoperative findings, Al-Mefty (1) classified posterior fossa meningiomas into six subtypes: petroclival, sphenopetroclival, clival, foramen magnum, anterior petrosal, and posterior petrosal. Petroclival meningiomas are defined as arising from the upper two thirds of the clivus, at the petroclival junction, and medial to the trigeminal nerve. Such tumors often span the middle and posterior cranial fossae and can involve the posterior cavernous sinus through Meckel cave. Sphenope-

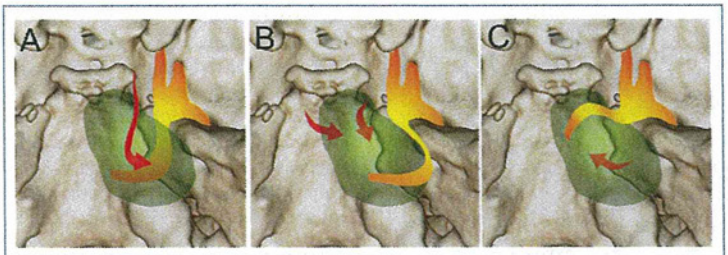

Figure 1. Schematic illustration of tumoral attachment and direction of trigeminal nerve displacement. **(A)** Trigeminal nerve is displaced caudally by tumor attached to tentorium (tentorial type). **(B)** Trigeminal nerve is displaced laterally by tumor attached to petroclival dura (petroclival type). **(C)** Trigeminal nerve is displaced rostrally by tumor attached to anterior petrous dura (anterior petrous type). Red arrows indicate the putative vascular supply of each attachment type.

troclival meningiomas are more extensive, involving the anterior cavernous sinus, invading the sella turcica and sphenoid sinus, and occasionally involving bilateral cavernous sinuses. Tumors arising from the midline clivus and displacing the brainstem and basilar artery posteriorly are defined as clival meningiomas, whereas tumors arising from the lower third of the clivus are defined as foramen magnum meningiomas. Posterior fossa meningiomas arising lateral to the trigeminal nerve are called petrosal meningiomas and are split into anterior and posterior petrosal meningiomas (1, 8). Tentorial meningiomas were not included in Al-Mefty's classification.

Operative mortality is increased mainly in association with cranial nerve injuries. To preserve the cranial nerves, the surgical field must be kept as bloodless as possible, and the cranial nerves need to be kept clear during surgical manipulation, even if deformed by the tumor. For this purpose, coagulating the feeding artery at the tumor attachment in the early stages of tumor resection is quite useful. A clear understanding of the relationship between the tumor attachment of the meningioma at the CPA and the cranial nerves is very important, particularly for the trigeminal nerve, because such knowledge can dramatically improve the speed and safety of the coagulation process. Meningiomas at the CPA usually grow slowly and have become large by the time of diagnosis, however, and are in contact with numerous surrounding neural, vascular, and bony structures. Knowing the precise location of the tumor attachment is sometimes difficult based on preoperative MRI alone (6, 14).

Cerebral angiography can be used to show the attachments of meningiomas because the vascular supply of these lesions comes from the normal dural arteries that supply the site of tumor attachment. Such arteries usually penetrate the meningioma peripherally and then develop an extensive arterial and capillary network in the center of the tumor (13), indicating that the feeding artery is well localized to the tumor attachment. With this concept, we hypothesized that angiographic classification corresponds to attachment classification and can be used to predict tumor attachment before surgery. The purpose of this study was to validate this hypothesis by retrospectively analyzing 34 cases of meningioma at the CPA treated surgically in our hospital.

METHODS

We studied 34 consecutive patients with meningioma at the CPA who underwent surgery at The University of Tokyo Hospital between November 2001 and April 2009. We included all meningiomas that extended into the CPA along the petroclival fissure or around the internal auditory meatus. We did not include meningiomas with obvious attachment to the lower clivus, jugular foramen, or foramen magnum or tentorial meningiomas unrelated to the CPA. Cases with previous surgical treatment were excluded because considerable alterations to tumor feeding would be present owing to the first operation. Mean age was 52 years (range 22–80 years), and the male-to-female ratio was 1:3 (9 men, 25 women). All study protocols were approved by the institutional review board.

Classification of the Attachment

Based on the operative records, attachment of the meningioma was classified into four types: tentorial, petroclival, anterior petrous, and posterior petrous. Tentorial type ($n = 13$) describes tumors attached to the dura mater from the tentorium to the anterior petrous bone. The trigeminal nerve is displaced caudally or medially. Petroclival type ($n = 7$) categorizes tumors attached medial to the trigeminal nerve. The trigeminal nerve is displaced laterally and is sometimes involved in the tumor. Anterior petrous type ($n = 6$) includes tumors arising from the dura mater of the anterior petrous bone or Meckel cave. The trigeminal nerve is displaced rostrally or medially. Posterior petrous type ($n = 8$) includes tumors with attachments that are posterior to the internal auditory meatus (including the

Figure 2. Axial **(A)** and coronal **(B)** views of magnetic resonance imaging (MRI) for posterior petrous type showed meningioma at the right cerebellopontine angle (CPA) attached to the posterior petrosal dura. The attachment was confirmed intraoperatively.

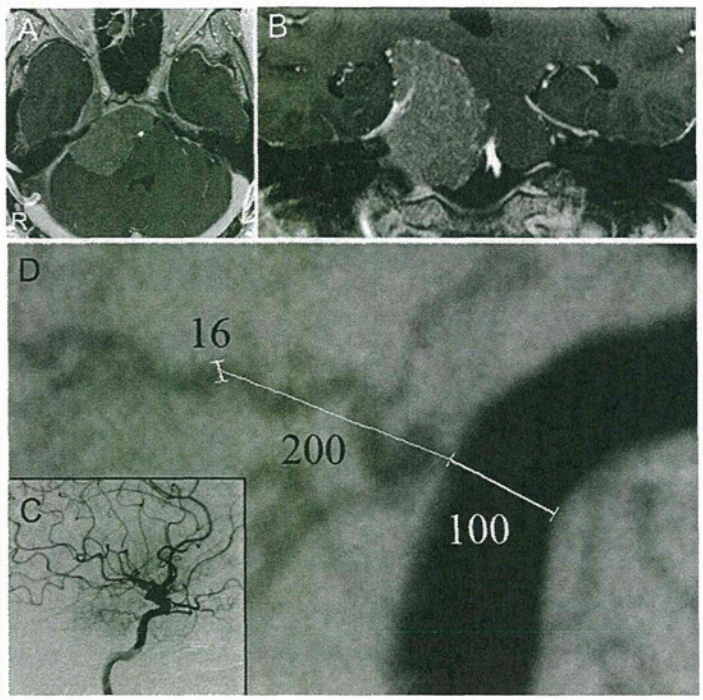

Figure 3. (A–C) Meningioma at the right cerebellopontine angle (CPA) growing in the petroclival region fed by an abnormally developed tentorial artery. **(D)** We defined the tentorial artery as "abnormally developed" when the caliber of the vessel was greater than 10% of internal carotid artery (ICA) caliber (caliber measured at double the length of the ICA away from its origin).

meatal wall and dorsal and ventral dura mater).

Of all the operative records, four records lacked clear description of tumor attachment. In seven other cases, it was difficult to decide the attachment type uniquely only by the direct description of tumor attachment. In these cases, we consulted the description on the direction of trigeminal nerve displacement (**Figure 1**). There were only four cases that lacked this information; three were posterior petrous type, and the other was a small tumor without any relationship with the trigeminal nerve in the operative field. All four cases had clear description of tumor attachment in the operative records. We made the classification of tumor attachment, which seemed to be reliable enough for the purpose of our study. We excluded posterior petrous type from further analysis because preoperative MRI was sufficient in all eight cases to predict the attachment of these tumors correctly (**Figure 2**).

Angiographic Findings

We considered the following two features the most decisive angiographic findings: abnormal development of the ipsilateral tentorial artery and tumor stain on contralateral internal carotid artery (ICA) angiography. The definition of abnormal development of the ipsilateral tentorial artery was as follows. We defined "a" as the caliber of the ICA at the bifurcation of the tentorial artery and "b" as the caliber of the tentorial artery at a distance of 2a from the ICA. If b/a was greater than 0.10 (ie, tentorial artery thicker than 10% of the ICA), the tentorial artery was considered to be abnormally developed. We excluded tentorial arteries that were shorter than 2a or originated from the ICA at an angle of less than 45 degrees (**Figure 3**). We determined the existence of tumor staining from the branches of the contralateral ICA only when identifiable in the arterial or capillary phase of contralateral ICA angiography. Two neurosurgeons independently interpreted angiographic findings.

Based on the above-described angiographic findings, tumors were classified into three angiographic types. Type A (abnormal ipsilateral tentorial artery type) includes tumors with abnormally developed ipsilateral tentorial artery. Type B (bilateral ICA type) includes tumors with staining of bilateral ICA angiograms. Type N (nontentorial, non-ICA type) includes tumors that lack features of type A and type B.

Table 1. Angiographic Classification

Type A (abnormal ipsilateral tentorial artery type)	Abnormally developed tentorial artery on ipsilateral ICA angiogram
Type B (bilateral ICA type)	Tumor stain on bilateral ICA angiograms
Type N (nontentorial, non-ICA type)	Lacking abnormally developed tentorial artery and bilateral tumor stain on ICA angiogram

ICA, internal carotid artery.

Table 2. Attachment Classification

Tentorial type	Trigeminal nerve shifted caudally/medially
	Attachment to tentorium
Petroclival type	Trigeminal nerve shifted laterally
Anterior petrous type	Trigeminal nerve shifted rostrally/medially
	Attachment to petrous apex

Table 3. Summary of Meningiomas at Cerebellopontine Angle

	Tentorial	Petroclival	Anterior Petrous	*P* Value
No. patients	13	7	6	
Age (years)	52.9	49.0	41.5	NS
Male (%)	30.8	14.3	66.7	NS
Size (mm)	38.5	40.1	40.2	NS
Presenting symptoms	Facial pain/numbness, 7	Gait disorder, 3	Decreased hearing, 3	
	Vertigo, 2	Double vision, 1	Hemiparesis, 2	
	Tinnitus, 2	Decreased hearing, 1	Facial pain/numbness, 2	
	Hemiparesis, 2	Hemiparesis, 1	Gait disorder, 1	
	Headache, 2	Tinnitus, 1	Tinnitus, 1	
	Dysarthria, 2	No symptoms, 2	No symptoms, 2	
	Double vision, 1			
Pathologic subtypes				
Meningothelial	9	6	2	
Fibrous	1	1	1	
Transitional	2	0	3	
Other	1	0	0	

NS, not significant ($P < 0.01$, one-way analysis of variance).

Statistical Analysis

Angiographic classification was compared with the attachment classification (**Tables 1** and **2**). The difference between these two classifications was analyzed with the χ^2 test with 4 degrees of freedom. Values of $P < 0.01$ were considered statistically significant. The κ statistic was subsequently used to calculate agreement between the two classifications, with each angiographic type paired to the corresponding attachment type in the order presented in **Tables 1** and **2**. The κ statistic is defined as the observed agreement divided by the agreement not accounted for by chance. Values of the κ statistic less than 0.4 represent slight to fair agreement, values between 0.4 and 0.6 indicate moderate agreement, values between 0.6 and 0.8 show substantial agreement, and values greater than 0.8 represent almost perfect agreement (7, 9, 17, 22). Sensitivity and specificity of each angiographic type were also calculated for the paired attachment type. Because small tumors were expected to lack sufficient tumor feeding to be detected by angiography, we defined tu-

Table 4. Contingency Table for All Tumors

	Tentorial	Petroclival	Anterior Petrous
Type A	10	0	0
Type B	0	4	1
Type N	3	3	5

χ^2 (4, n = 26) = 21.3, $P < .01$.
κ statistic = 0.59 (95% confidence interval [CI] 0.35–0.83).

Table 5. Contingency Table for Large Tumors (>30 mm)

	Tentorial	Petroclival	Anterior Petrous
Type A	9	0	0
Type B	0	4	1
Type N	0	1	4

χ^2 (4, n = 19) = 25.8, $P < .01$.
κ statistic = 0.83 (95% CI 0.62–1).

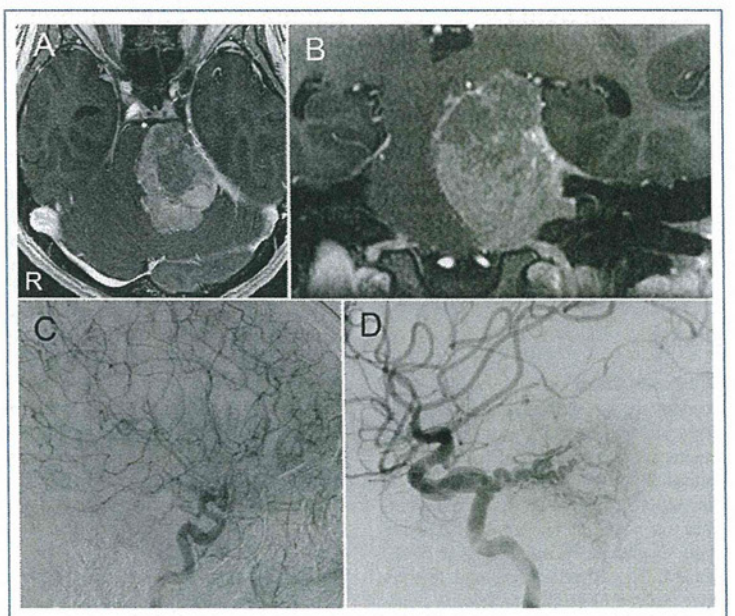

Figure 4. Axial **(A)** and coronal **(B)** views of magnetic resonance imaging (MRI) and lateral views of right **(C)** and left **(D)** internal carotid artery (ICA) angiography for tentorial type. Meningioma at the left cerebellopontine angle (CPA) fed by an abnormally developed tentorial artery was intraoperatively revealed to have an attachment to the medial tentorium. No significant tumor stain is evident on contralateral ICA angiography **(C)**.

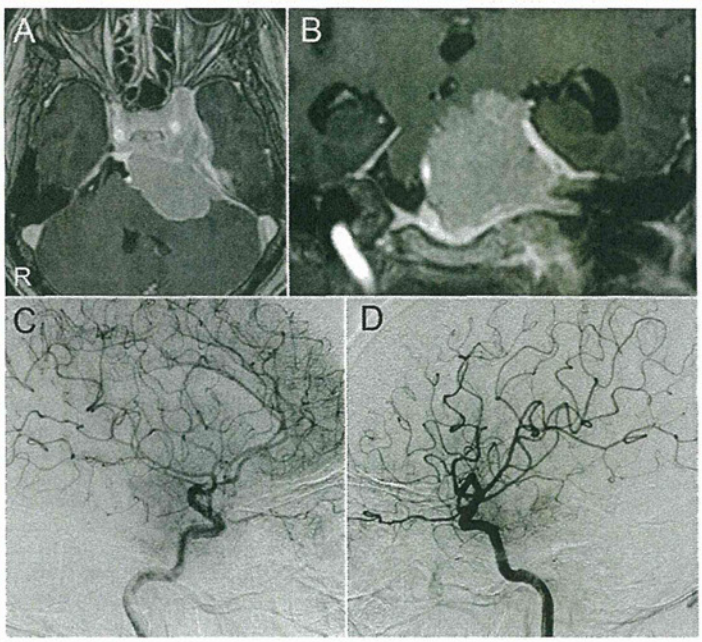

Figure 5. Axial **(A)** and coronal **(B)** views of magnetic resonance imaging (MRI) and lateral views of right **(C)** and left **(D)** internal carotid artery (ICA) angiography for petroclival type. Meningioma at the left cerebellopontine angle (CPA) with tumor stain from bilateral ICA angiograms **(C** and **D)** was intraoperatively revealed to push the trigeminal nerve laterally and to have a main attachment to the petroclival dura.

mors greater than 30 mm as an optimal subgroup for this study and separately calculated its statistical parameters. All statistical analyses were performed using JMP (version 8.0; SAS Institute, Cary, North Carolina, USA).

RESULTS

Attachment Classification

Every tumor was classified into one of the three attachment types in a compatible manner. The proportion of male patients tended to be slightly higher with the anterior petrous type, but no significant difference was noted. All tumors showed pathologic diagnoses corresponding to WHO grade I. No particular pathologic features were evident. Regarding presenting symptoms, trigeminal neuropathy, including facial pain or numbness, was most common in the tentorial type. In the petroclival type, gait disturbance was most frequent, and trigeminal neuropathy was absent (**Table 3**).

Angiographic Classification

All tumors were successfully classified into one of the three angiographic types. Although angiographic features such as abnormal ipsilateral tentorial artery and contralateral ICA staining are theoretically compatible, there was no tumor that satisfied both of these criteria simultaneously. There was no correlation between angiographic features and pathologic subtypes.

There was no significant complication of angiography, which was performed by trained radiologists and neurosurgeons. No prolonged hospitalization was required in association with the procedure.

Comparison Between Two Classifications

The χ^2 test for independence indicated a significant relationship between attachment classification and angiographic classification (χ^2 [4, n = 26] = 21.3; P < 0.01). κ statistic was 0.59 (95% confidence interval [CI] 0.35–0.83), indicating moderate agreement between the classifications (**Table 4**). For tumors greater than 30 mm in diameter, κ statistic was 0.83 (95% CI 0.62–1.0), indicating almost complete agreement between classifications (**Table 5**).

For the 13 tumors with tentorial-type attachment, 10 tumors showed type A angiographic features (**Figure 4**). Sensitivity and specificity of type A for tentorial type were 76.9% and 100%. Among seven tumors with petroclival-type attachment, four had type B angiographic features (**Figure 5**). Sensitivity and specificity of type B for petroclival type were 57.1% and 94.7%. In particular, tumors 30 mm or less in diameter showed no tumor staining. As a result, tumors greater than 30 mm showed a higher sensitivity of 80.0%. Among six tumors with anterior petrous–type attachment, five showed type N angiographic features, and one tumor had type A features (**Figure 6**). Sensitivity and specificity of type N for anterior petrous type were 83.3% and 70%. Tumors greater than 30 mm in diameter showed a higher specificity of 92.9% (**Table 6**).

Correlation Between Findings of Magnetic Resonance Imaging and Attachment Classification

The close inspection of MRI (including T1-weighted images, T2-weighted images, and fast imaging employing steady-state acquisition [FIESTA] images with or without enhancement) provided us with detailed information not only on extent, consistency, and precise position of the tumor, but also on other surrounding structures, such as blood vessels including arteries and veins, several nerves, and the brainstem, allowing the spatial relationship between these structures to be visualized. As described earlier, all the tumors of posterior petrous type were correctly classified as such by MRI. We were unable to predict attachment of most tumors by MRI alone, however, because large tumors showed a wide range of contacts with surrounding structures, and characteristic signs such as bone hypertrophy were not frequently evident. We investigated a subgroup of tumors 30 mm or less in diameter. Some of these tumors were small enough to have definite attachment recognizable from inspection of MRI. Attachment type was obvious in four of seven tumors in this subgroup. Two tumors were

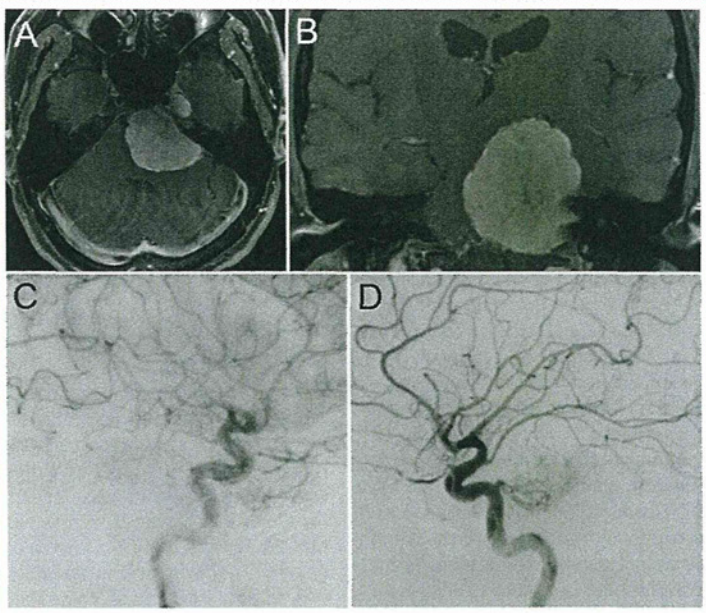

Figure 6. Axial **(A)** and coronal **(B)** views of magnetic resonance imaging (MRI) and lateral views of right **(C)** and left **(D)** internal carotid artery (ICA) angiography for anterior petrous type. Meningioma at the left cerebellopontine angle (CPA) fed by several small branches (e.g., medial or lateral clival arteries, not tentorial artery) from the ICA was intraoperatively revealed to have a main attachment to the petrous apex dura. No significant tumor stain is evident on contralateral ICA angiography **(C)**.

tentorial type, and another two were petroclival type.

DISCUSSION

This study showed that angiographic findings are useful for classifying the attachment of meningiomas at the CPA. Generally, angiographic type A corresponds to tentorial type in attachment classification, type B corresponds to petroclival type, and type N corresponds to anterior petrous type. In particular, in cases with tumors greater than 30 mm in diameter, these paired classifications showed complete correspondence. In addition, sensitivity and specificity of our angiographic classification for the paired attachment classification were greater than 80%. Angiographic findings are strongly correlated with attachment classification, whereas it is difficult to know the attachment of meningiomas at the CPA by MRI alone.

Meningiomas at the CPA or in the petroclival region have been classified variously based on intraoperative findings, and a systematically formulated nomenclature has been lacking. Meningiomas originating from the medial rim of the tentorium have sometimes been discussed as tentorial meningiomas (6, 31). We propose dealing with these discretely defined meningiomas as a unique spectrum of tumors occupying the CPA and classifying these tumors into three types based on the direction of trigeminal nerve displacement. This classification of attachments seems to show sufficient concordance with classification based on the angiographic feeding artery and supplies useful information for deciding appropriate surgical procedures.

We selected two angiographic features as decisive findings. One was tumor stain from the contralateral ICA, and the other was presence of an abnormally developed tentorial artery. These features were selected based on the anatomic considerations described subsequently. The petroclival dura mater is fed by the medial or lateral clival artery, and the tentorium is fed by the tentorial artery. Because the tentorial artery runs along the medial rim of the tentorium and then feeds the tumor, a tumor originating from the petroclival dura mater is unlikely to receive blood supply from the tentorial artery. The clival artery shows a complicated anastomosis with branches of the ICA or ascending pharyngeal artery and shows right and left anastomoses in the midst of the clivus physiologically (24), making it possible that tumors attached to the clivus could show angiographic tumor staining from the contralateral ICA. Anterior petrous meningiomas, without attachment to the tentorium or clivus, should lack both features. This is why we paired the two classifications as described earlier. Small tumors are sometimes classified as type N (nontentorial, non-ICA type), and the predicted attachments tend to be to the dura mater of the anterior petrous bone. Actually, in cases of tumors 30 mm or less in size, the false-positive rate of angiographic

Table 6. Summary of Sensitivity and Specificity

Angiographic Type for Paired Attachment Type	All Tumors		Large Tumors (>30 mm)	
	Sensitivity (%)	Specificity (%)	Sensitivity (%)	Specificity (%)
Type A for tentorial type	76.9	100.0	100.0	100.0
Type B for petroclival type	57.1	94.7	80.0	92.9
Type N for anterior petrous type	83.3	70.0	80.0	92.9

type N for anterior petrous type in the attachment classification is increased. Predicting the attachment of such small tumors by preoperative MRI alone was not difficult, however. Applying this angiographic classification to tumors greater than 30 mm seems practical. In comparison, the sensitivity of type A (abnormal ipsilateral tentorial artery type) is sufficiently high even for small tumors (≤30 mm), indicating that an abnormally developed tentorial artery represents a quite sensitive index. Although the hypertrophic tentorial artery of Bernasconi and Cassinari in tentorial meningioma has been known for decades, tentorial meningiomas have not been discussed within the context of posterior fossa meningiomas. In this sense, it seems meaningful to emphasize that meningiomas fed by abnormally developed tentorial arteries constitute a substantial number of meningiomas at the CPA.

One of the benefits of knowing the attachment preoperatively is that the most effective surgical approach can be selected. Sometimes it is difficult to embolize the feeding artery of meningiomas at the CPA preoperatively because of dangerous anastomoses and risk of ischemic injuries to the cranial nerves (12). It is crucial to obstruct the feeder in the early stage of the surgery. If we know the tumor attachment, we can approach the attachment directly, detach it by coagulation, and cauterize the feeding arteries. For tumors attached to the tentorium, a direct approach to the inferior surface of the tentorium is desirable to detach the tumor. A retrosigmoid approach is sufficient for tumors without massive supratentorial extension (14). If the tumor is attached to the petroclival dura, the posterior petrosal approach needs to be combined with various extents of anterior petrosectomy (8). If the attachment is localized to the anterior petrous dura, a retrosigmoid approach is enough for such a small tumor. For the purposes of preserving serviceable hearing, a petrosal approach is considered more suitable (5, 8, 14).

Another benefit of predicting the tumor attachment is that the direction of trigeminal nerve displacement can be determined. In the case of petroclival type, surgeons can pay special attention not to injure the trigeminal nerve, which is located immediately beneath the petrous bone and the tentorium (14). Knowing the location of cranial nerves enables the tumor attachment to be handled quickly and the surgical field to be kept bloodless, allowing better preservation of cranial nerves. The relationship between the tumor and cranial nerves can also be shown by MRI cisternography with contrast enhancement, such as FIESTA or constructive interference in the steady state (21). These methods are not always successful, however, especially in cases of large tumors, because cranial nerves are very small structures and are sometimes stretched or otherwise changed by tumoral involvements. At the very least, angiographic diagnosis of the tumor attachment offers confirmation of cranial nerve displacement.

It is impractical to perform angiography in all cases of meningiomas at the CPA. At the present time, however, angiography offers the most reliable information on the feeding patterns of these lesions for the following reasons. First, angiography has hemodynamic information that enables one to detect not only feeding arteries in the arterial phase but also tumor staining in the capillary phase. Second, although other modalities, such as magnetic resonance angiography (MRA) or three-dimensional computed tomography angiography (CTA), are useful to detect relatively large structures, such as normal-sized aneurysm (10, 23), their ability to delineate small feeding arteries remains to be established owing to their insufficient resolution and partial volume effect (15). The result of this study in itself can be used in the future when MRA or three-dimensional CTA overcomes these limitations. From that perspective, we have successfully shown the fundamental concept in developing the operative strategy for meningiomas in this location. If the feeding arteries could be finely depicted three-dimensionally, operative strategies would be more readily discussed based on three-dimensional images illustrating structural interactions. We derived the idea for this study in the process of preparing three-dimensional images showing structures around the tumors.

This study has several limitations. The retrospective nature of this study and the relatively small sample size necessitate further validation of the present findings. Some of the operative records that we used as the standard references had incomplete information of tumor attachment, diminishing the reliability of this study. The practical utility of our angiographic classification is limited because angiography is no longer considered essential to preoperative assessment of meningioma surgery. Future studies are needed comparing less invasive modalities such as MRA or three-dimensional CTA with conventional angiography. Despite these limitations, the contribution of our findings is primarily in proposing the angiographic prediction of the tumor attachment, which has not previously been reported and has a great impact on treating meningioma at the CPA.

CONCLUSIONS

We showed that our angiographic classification has a strong correspondence with the attachment classification in cases of large tumors (>30 mm). This correspondence allows preoperative determination of the tumor attachment of meningiomas at the CPA. We have discussed the clinical importance of this method in selecting optimal surgical strategies for these challenging lesions.

REFERENCES

1. Al-Mefty O: Operative Atlas of Meningiomas. Philadelphia: Lippincott-Raven; 1998.
2. Al-Mefty O, Fox JL, Smith RR: Petrosal approach for petroclival meningiomas. Neurosurgery 22:510-517, 1988.
3. Bricolo AP, Turazzi S, Talacchi A, Cristofori L: Microsurgical removal of petroclival meningiomas: a report of 33 patients. Neurosurgery 31:813-828, 1992.
4. Chen TC, Zee CS, Miller CA, Weiss MH, Tang G, Chin L, Levy ML, Apuzzo ML: Magnetic resonance imaging and pathological correlates of meningiomas. Neurosurgery 31:1015-1021, 1992.
5. Cho CW, Al-Mefty O: Combined petrosal approach to petroclival meningiomas. Neurosurgery 51:708-716, 2002.
6. Colli BO, Assirati JA Jr, Deriggi DJ, Neder L, dos Santos AC, Carlotti CG Jr: Tentorial meningiomas: follow-up review. Neurosurg Rev 31:421-430, 2008.
7. Elmore JG, Wells CK, Lee CH, Howard DH, Feinstein AR: Variability in radiologists' interpretations of mammograms. N Engl J Med 331:1493-1499, 1994.
8. Erkmen K, Pravdenkova S, Al-Mefty O: Surgical management of petroclival meningiomas: factors determining the choice of approach. Neurosurg Focus 19:E7, 2005.

9. Fleiss JL: Statistical Methods of Rates and Proportions, 2nd ed. New York: John Wiley; 1981.

10. Franklin B, Gasco J, Uribe T, Vonritschl RH, Hauck E: Diagnostic accuracy and inter-rater reliability of 64-multislice 3D-CTA compared to intra-arterial DSA for intracranial aneurysms. J Clin Neurosci 17: 579-583, 2010.

11. Hakuba A, Nishimura S, Tanaka K, Kishi H, Nakamura T: Clivus meningioma: six cases of total removal. Neurol Med Chir (Tokyo) 17(1 Pt 1):63-77, 1977.

12. Hirohata M, Abe T, Morimitsu H, Fujimura N, Shigemori M, Norbash AM: Preoperative selective internal carotid artery dural branch embolisation for petroclival meningiomas. Neuroradiology 45:656-660, 2003.

13. Huber P: Cerebral Angiography. New York: Thieme Stratton; 1982.

14. Ichimura S, Kawase T, Onozuka S, Yoshida K, Ohira T: Four subtypes of petroclival meningiomas: differences in symptoms and operative findings using the anterior transpetrosal approach. Acta Neurochir (Wien) 150:637-645, 2008.

15. Kato Y, Sano H, Katada K, Ogura Y, Hayakawa M, Kanaoka N, Kanno T: Application of three-dimensional CT angiography (3D-CTA) to cerebral aneurysms. Surg Neurol 52:113-121, 1999.

16. Kawase T, Shiobara R, Ohira T, Toya S: Developmental patterns and characteristic symptoms of petroclival meningiomas. Neurol Med Chir (Tokyo) 36: 1-6, 1996.

17. Landis JR, Koch GG: The measurement of observer agreement for categorical data. Biometrics 33:159-174, 1977.

18. Little KM, Friedman AH, Sampson JH, Wanibuchi M, Fukushima T: Surgical management of petroclival meningiomas: defining resection goals based on risk of neurological morbidity and tumor recurrence rates in 137 patients. Neurosurgery 56:546-559, 2005.

19. Maiuri F, Iaconetta G, de Divitiis O, Cirillo S, Di Salle F, De Caro ML: Intracranial meningiomas: correlations between MR imaging and histology. Eur J Radiol 31:69-75, 1999.

20. Mayberg MR, Symon L: Meningiomas of the clivus and apical petrous bone: report of 35 cases. J Neurosurg 65:160-167, 1986.

21. Mikami T, Minamida Y, Yamaki T, Koyanagi I, Nonaka T, Houkin K: Cranial nerve assessment in posterior fossa tumors with fast imaging employing steady-state acquisition (FIESTA). Neurosurg Rev 28:261-266, 2005.

22. Oudkerk M, van Beek EJ, Wielopolski P, van Ooijen PM, Brouwers-Kuyper EM, Bongaerts AH, Berghout A: Comparison of contrast-enhanced magnetic resonance angiography and conventional pulmonary angiography for the diagnosis of pulmonary embolism: a prospective study. Lancet 359:1643-1647, 2002.

23. Piotin M, Gailloud P, Bidaut L, Mandai S, Muster M, Moret J, Rufenacht DA: CT angiography, MR angiography and rotational digital subtraction angiography for volumetric assessment of intracranial aneurysms: an experimental study. Neuroradiology 45:404-409, 2003.

24. Salamon GM, Combalbert A, Raybaud C, Gonzalez J: An angiographic study of meningiomas of the posterior fossa. J Neurosurg 35:731-741, 1971.

25. Sekhar LN, Jannetta PJ, Burkhart LE, Janosky JE: Meningiomas involving the clivus: a six-year experience with 41 patients. Neurosurgery 27:764-781, 1990.

26. Sekhar LN, Wright DC, Richardson R, Monacci W: Petroclival and foramen magnum meningiomas: surgical approaches and pitfalls. J Neurooncol 29: 249-259, 1996.

27. Spallone A, Makhmudov UB, Mukhamedjanov DJ, Tcherekajev VA: Petroclival meningioma: An attempt to define the role of skull base approaches in their surgical management. Surg Neurol 51:412-419, 1999.

28. Spetzler RF, Daspit CP, Pappas CT: The combined supra- and infratentorial approach for lesions of the petrous and clival regions: experience with 46 cases. J Neurosurg 76:588-599, 1992.

29. Suzuki Y, Sugimoto T, Shibuya M, Sugita K, Patel SJ: Meningiomas: correlation between MRI characteristics and operative findings including consistency. Acta Neurochir (Wien) 129:39-46, 1994.

30. Yamaguchi N, Kawase T, Sagoh M, Ohira T, Shiga H, Toya S: Prediction of consistency of meningiomas with preoperative magnetic resonance imaging. Surg Neurol 48:579-583, 1997.

31. Yasargil MG: Microneurosurgery of CNS Tumors, vol. 4B. Stuttgart: Thieme; 1996.

32. Yasargil MG, Mortara RW, Curcic M: Meningioma of basal posterior cranial fossa. In: Krayenbühl H, ed. Advances and Technical Standards in Neurosurgery. Vienna: Springer-Verlag; 1980:1-115.

33. Yoneoka Y, Fujii Y, Takahashi H, Nakada T: Preoperative histopathological evaluation of meningiomas by 3 0T T2R MRI. Acta Neurochir (Wien) 144: 953-957, 2002.

Conflict of interest statement: The authors declare that the article content was composed in the absence of any commercial or financial relationships that could be construed as a potential conflict of interest.

received 1 February 2010; accepted 17 September 2010

Citation: World Neurosurg. (2011) 75, 1:114-121.
DOI: 10.1016/j.wneu.2010.09.020

Journal homepage: www.WORLDNEUROSURGERY.org

Available online: www.sciencedirect.com

1878-8750/$ - see front matter

18) Tos M, Trojaborg N, Thomsen J: The contralateral ear after translabyrinthine removal of acoustic neuromas: is there a drill-noise generated hearing loss? *J Laryngol Otol* 103: 845-849, 1989
19) van Veelen-Vincent ML, Delwel EJ, Teeuw R, Kurt E, de Jong DA, Brocaar MP, Pauw BK, Avezaat CJ, van Zanten BG: Analysis of hearing loss after shunt placement in patients with normal-pressure hydrocephalus. J Neurosurg 95: 432-434, 2001
20) Walsh RM, Murty GE, Punt JA, O'Donoghue GM: Sudden contralateral deafness following cerebellopontine angle tumor surgery. *Am J Otol* 15: 244-246, 1994
21) Walsted A, Salomon G, Thomsen J, Tos M: Cerebrospinal fluid loss and threshold changes. 1. Hearing loss in the contralateral ear after operation for acoustic neuroma: an analysis of the incidence, time course, frequency range, size and pathophysiological considerations. *Audiol Neurootol* 1: 247-255, 1996
22) Wlodyka J: Studies on cochlear aqueduct patency. *Ann Otol Rhinol Laryngol* 87(1 Pt 1): 22-28, 1978

Address reprint requests to: Takashi Shuto, MD, Department of Neurosurgery, Yokohama Rosai Hospital, 3211 Kozukue-cho, Kouhoku-ku, Yokohama, Kanagawa 222-0036, Japan. *e-mail*: shuto@yokohamah.rofuku.go.jp

Neurol Med Chir (Tokyo) 51, 437~441, 2011

Hydrocephalus Due to Diffuse Villous Hyperplasia of the Choroid Plexus

—Case Report—

Ryogo ANEI,[1] Yoshimitsu HAYASHI,[1] Satoru HIROSHIMA,[1] Nobuyuki MITSUI,[1] Ryosuke ORIMOTO,[1] Genki UEMORI,[1] Masato SAITO,[1] Masao SATO,[1] Hajime WADA,[1] Akira HODODUKA,[1] and Kyousuke KAMADA[1]

[1]*Department of Neurosurgery, Asahikawa Medical College, Asahikawa, Hokkaido*

Abstract

An 8-month-old female presented with hydrocephalus caused by cerebrospinal fluid (CSF) overproduction due to bilateral choroid plexus enlargement, which was clinically diagnosed as diffuse villous hyperplasia of the choroid plexus, but differentiation from bilateral choroid plexus papilloma was difficult. She initially underwent ventriculoperitoneal shunt surgery, but developed marked retention of ascites. Therefore, the peritoneal end of the shunt was removed for external drainage, but excessive CSF (1,500 ml/day) was collected. Computed tomography and magnetic resonance imaging revealed marked symmetric enhancement of the choroid plexuses in the bilateral lateral ventricles. Thallium-201 chloride single-photon emission computed tomography showed pronounced uptake on both early and delayed images, and good washout. CSF examination revealed no abnormalities such as atypical cells, and a ventriculoatrial shunt was inserted, achieving good control of the hydrocephalus.

Key words: choroid plexus, hyperplasia, hydrocephalus, cerebrospinal fluid overproduction, ventriculoatrial shunt

Introduction

Diffuse villous hyperplasia of the choroid plexus (DVHCP) is a rare condition involving enlargement of the entire choroid plexus, which remains histologically normal, resulting in severe hydrocephalus due to cerebrospinal fluid (CSF) overproduction. DVHCP must be differentiated from the rare occurrence of bilateral choroid plexus papilloma (CPP), but discrimination between the two diseases still presents problems. We treated a patient under a diagnosis of DVHCP based on clinical findings, but differentiation from bilateral CPP was difficult due to the lack of pathological specimens.

Received April 30, 2010; Accepted October 18, 2010

Case Report

An 8-month-old female was brought to our hospital as an emergency case from a local hospital due to an acute increase in her head circumference, tightness of the lower limbs, and poor sucking ability on September 30, 2009. She was born in distress by Caesarian section on the 4th day of the 34th week of pregnancy in December 2008. Computed tomography (CT) showed intraventricular bleeding and hydrocephalus, but she was discharged after 1 month, and she was observed on an outpatient basis. After about 2 months, she developed tightness of the lower limbs, gradually lost energy, and demonstrated poor sucking reflex, so she was taken to another hospital. Since emergency magnetic resonance (MR) imaging revealed marked hydrocephalus, she was transported to our hospital.

On admission, her head circumference was 49.5 cm (> +2 standard deviation), compared to 43.1 cm 1 month earlier. The anterior fontanelle was tense, and sunset phenomenon, tightness of the lower limbs, and scalp vein distention were observed. Heart rate, respiratory rate, blood pressure, and body temperature were normal. Blood examination showed no abnormalities in any parameter including electrolytes, renal function, and liver function. CT revealed marked ventricular dilation and periventricular lucency (Fig. 1).

Emergency ventriculoperitoneal (VP) shunt surgery was performed. The surgical procedure was completed without problems. On the day following the operation, marked abdominal distention occurred. Abdominal CT revealed massive accumulation of free fluid in the abdominal cavity (Fig. 2). We considered that her peritoneum could not adequately absorb the CSF, and removed the peritoneal end of the shunt to allow external drainage. The initial pressure was established at 100 mm above the patient's external acoustic meatus. Since 200 ml CSF/hour drained from the external acoustic meatus, intermittent clamping was performed to prevent excessive outflow. However, 200 ml CSF/hour continued to drain. CSF examination showed no abnormal values or atypical cells.

CT and MR imaging, both with contrast medium, showed prominent enhancement of the symmetrically enlarged bilateral choroid plexuses (Fig. 3). Thallium-201 chloride single-photon emission computed tomography (Tl SPECT) revealed marked uptake on both early and delayed images and good washout with a negative retention index (Fig. 4). After 2 weeks, her general condition worsened, with hyponatremia, methicillin-resistant *Staphylococcus aureus* pneumonia, and meningitis, prompting performance of a tracheotomy. However, improvement was observed after antibiotic administration intravenously and into the CSF. The diagnostic significance of the Tl SPECT was unclear at this point, but

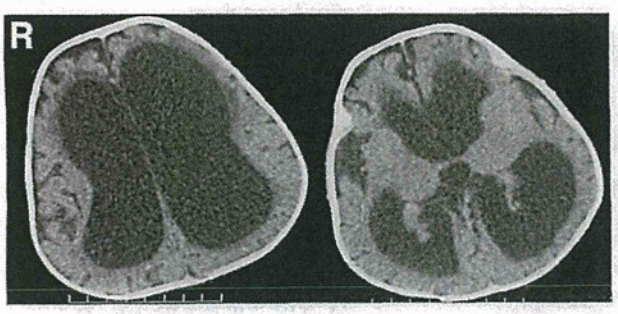

Fig. 1 Computed tomography scans on admission showing marked ventricular dilation and periventricular lucency.

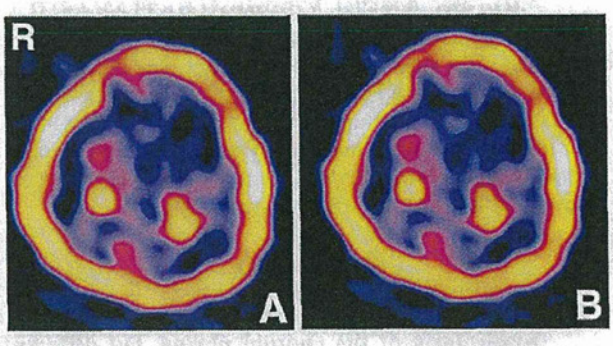

Fig. 4 Thallium-201 chloride single-photon emission computed tomography scans showing marked uptake (tumor to nontumorous brain ratio) on both early (A: right 11.81, left 13.68) and delayed images (B: right 3.08, left 3.09), and negative retention index (right −73.91, left −77.4), suggesting good washout.

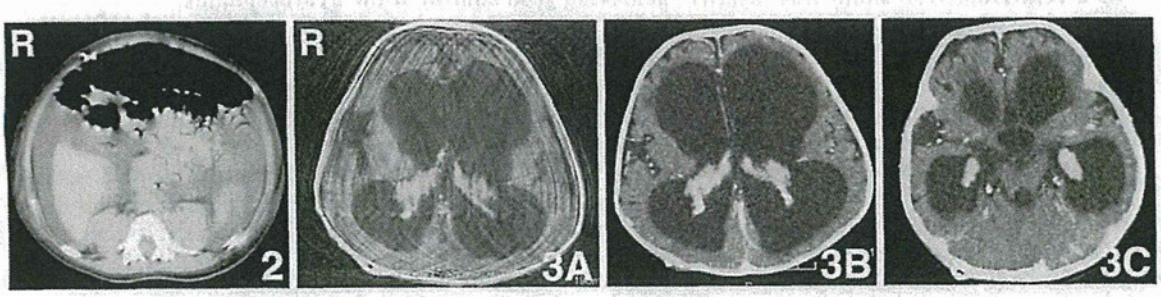

Fig. 2 Abdominal computed tomography scan on the day after the first operation revealing massive free fluid in the peritoneum.
Fig. 3 T_1-weighted magnetic resonance image (A) and computed tomography scans (B, C) with contrast medium showing no mass lesion, but the markedly enhanced bilateral choroid plexuses.

Table 1 Cases of bilateral choroid plexus papilloma and diffuse villous hyperplasia of the choroid plexus (DVHCP)

Author (Year)	Age at initial procedure	Radiographical features	Initial (and 2nd) procedures	Last procedure	Clinical diagnosis	Histological findings
Gudeman et al. (1979)[12]	3 yrs	SE	VPS, VAS	resection	papilloma	papilloma
Welch et al. (1983)[22]	7 yrs	SE	VPS	resection	DVHCP	NCP
Bucholz and Pittman (1991)[3]	29 mos	SE	VPS	EC	DVHCP	NCP
Hirano et al. (1994)[13]	7 yrs	SE	VPS	resection	DVHCP	NCP
Britz et al. (1996)[2]	3 mos	SE	VPS	VAS	DVHCP	no
Philips et al. (1998)[16]	14 mos	SE, CF	VPS	EC, VPS	DVHCP	NCP
Fujimura et al. (2001)[11]	10 mos	SE, lobular	VPS, VAS	resection	papilloma	papilloma
Erman et al. (2003)[8]	3 yrs	ASE, lobular	resection	(resection)	papilloma	papilloma
D'Ambrosio et al. (2003)[7]	3 mos	SE	VPS	resection	DVHCP	NCP
Fujimoto et al. (2004)[10]	20 mos	SE	VPS	resection	DVHCP	NCP
Aziz et al. (2005)[1]	11 yrs	SE	VPS (at 2 mos)	resection	DVHCP	NCP
Tamburrini et al. (2006)[19]	24 mos	SE	VPS	EC, resection, VPS	DVHCP	NCP
Iplikcioglu et al. (2006)[14]	5 yrs	SE	VPS	VAS	DVHCP	no
Smith et al. (2007)[18]	15 mos	SE	VPS	resection, VPS	DVHCP	NCP
Warren et al. (2009)[21]	8 days	SE, irregular	VPS	resection, VPS	DVHCP	NCP
Nimjee et al. (2010)[15]	6 mos	ASE, CF	VPS, VAS	resection	papilloma	papilloma
Cataltepe et al. (2010)[5]	9 days	SE	VPS, EC	resection, VPS, VAS	DVHCP	NCP
Present case	8 mos	SE	VPS	VAS	DVHCP?	no

ASE: asymmetrical enlargement, CF: cyst formation, EC: endoscopic coagulation, NCP: normal choroid plexus, SE: symmetrical enlargement, VAS: ventriculoatrial shunt, VPS: ventriculoperitoneal shunt.

DVHCP was the most likely diagnosis based on the CT, MR imaging, and CSF findings. After resolution of the meningitis, a ventriculoatrial (VA) shunt was inserted.

She was transferred to the previous referring hospital, and has been followed up on an outpatient basis. Her intracranial pressure has been well controlled. No morphological changes were observed in the bilateral plexuses on follow-up CT 6 months after the operation.

Discussion

DVHCP was first reported by Davis[6] in 1924 before the introduction of CT, and only 18 patients with hydrocephalus caused by CSF overproduction due to bilateral choroid plexus enlargement have been reported, including findings employing imaging techniques (Table 1).[1-3,5,7,9-16,18,19,21,22] In most patients, VP shunt surgery was performed but failed, resulting in marked ascites. This suggests difficulty in establishing the diagnosis of this disease in the initial stage.

Bilateral CPP is characterized by asymmetric enlarged choroid plexuses[9,15] which tend to be separated into lobules,[9,11] and cyst formation in a few cases.[15] However, the enlarged choroid plexuses were symmetric and resembled DVHCP on imaging in some cases,[12] enabling diagnosis only after pathological examination. Most patients diagnosed with DVHCP[1-3,5,7,10,13,14,16,18,19,21,22] showed symmetric choroid plexus enlargement, but some exhibited irregular enlargement[21] or cyst formation.[6] In addition, no pathological findings were available in 3 patients including our patient, so the diagnosis of DVHCP was based on imaging findings.[3,14] Differential diagnosis is possible based on imaging findings,[14] and VA shunt surgery is the simplest and most appropriate choice,[22] considering the risks of complications of resection such as hemianopsia, nystagmus, and bleeding during the operation due to the rich blood flow in the choroid.[15,19] Indeed, 3-year follow-up examination showed good control of hydrocephalus and absence of morphological changes in the choroid plexus in previous patients.[2,14] Similar results were obtained in our patient, although the follow-up period was only 6 months. We also evaluated other options (biopsy or resection), but selected VA shunt without biopsy and resection, considering the risks of shunt failure due to bleeding-related increase in the CSF protein level when a shunt becomes necessary, infection due to long-term external drainage, and electrolyte abnormalities due to the removal of a large volume of CSF from the body.[3] However, pathological findings may be needed to establish the diagnosis.[9,11] Initial VA shunt was subsequently followed by tissue resection and pathological examination due to the development of complications such as thrombosis and infection, resulting in the diagnosis of bilateral CPP.[11,15] In most previous patients, the diagnosis of DVHCP was established based on the histological findings.[1,3,5,7,10,13,16,18,19,21,22] However, pathological examination suggested DVHCP on the tissue surface but CPP in the lobular lesion, confounding the pathological diagnosis of DVHCP in one case.[11]

Tl SPECT observed symmetric, marked uptake in the bilateral choroid plexuses on both early and delayed images and good washout, showing a negative retention index in our patient (Fig. 4). Tl SPECT in a patient with unilateral lateral ventricular CPP observed marked uptake in the CPP on the affected side on both early and delayed images and a retention index of −0.15, indicating moderate washout, but no uptake in the choroid plexus on the unaffected side.[17] Although the CT and MR imaging find-

ings suggested DVHCP in our patient, CPP remains a possibility. Therefore, long-term follow-up observation is necessary despite the absence of morphological changes after 6 months.

DVHCP may progress to CPP and finally to choroid plexus carcinoma (CPC), suggesting the importance of measuring the MIB-1 index.[7] The MIB-1 index is nearly 0% in the normal choroid plexus, 0.2–17.42% in CPP, and 4.14–29.74% in CPC.[4,6,20] The MIB-1 index was 4% in a previous case,[7] and 3% (left) and 0.5% (right) in another case,[5] suggesting the transition period from DVHCP to CPP in both patients. The pathological condition may have reflected this transition from DVHCP to CPP in patients with histological findings differing between specimen sites,[11] atypical imaging findings for pathological findings,[16,21] or uptake on Tl SPECT despite DVHCP suggested by CT and MR imaging, as in our patient.

In the majority of patients[2,3,5,7,10–16,18,19,21,22] including ours, VP shunt surgery was performed first, but failed due to marked ascites. Subsequently, resection or endoscopic coagulation was performed in most patients to inhibit CSF production, followed by radical or shunt surgery.[1,3,5,7,10–13,15,16,18,19,21,22] The advantage of these procedures is that histological diagnosis is possible, so CPP is not overlooked. However, the histological findings may differ between sites, which causes confusion.[11] In addition, there are risks of neurological complications,[22] and adverse effects of invasiveness, such as bleeding.[21] On the other hand, a method in which excessive CSF is returned to the systemic circulation using a VA shunt has been proposed,[14] which is noninvasive and straightforward, but whether the direct return of a large volume of CSF to the systemic circulation is appropriate remains questionable. The most important disadvantage is that definite histological diagnosis cannot be established. In our patient, excessive CSF was also directly returned to the systemic circulation using a VA shunt, but long-term follow-up observation is necessary.

The present and previous cases of hydrocephalus caused by CSF overproduction due to bilateral choroid plexus enlargement considered to be DVHCP suggest that a full disease description, diagnostic criteria, and treatment methods have not yet been established, requiring further studies.

References

1) Aziz AA, Coleman L, Morokoff A, Maixner W: Diffuse choroid plexus hyperplasia: an under-diagnosed cause of hydrocephalus in children? *Pediatr Radiol* 35: 815–818, 2005
2) Britz GW, Kim DK, Loeser JD: Hydrocephalus secondary to diffuse villous hyperplasia of the choroid plexus. Case report and review of the literature. *J Neurosurg* 85: 689–691, 1996
3) Bucholz RD, Pittman T: Endoscopic coagulation of the choroid plexus using the Nd:YAG laser: initial experience and proposal for management. *Neurosurgery* 28: 421–427, 1991
4) Carlotti CG Jr, Salhia B, Weitzman S, Greenberg M, Dirks PB, Mason W, Becker LE, Rutka JT: Evaluation of proliferative index and cell cycle protein expression in choroid plexus tumors in children. *Acta Neuropathol* 103: 1–10, 2002
5) Cataltepe O, Liptzin D, Jolley L, Smith TW: Diffuse villous hyperplasia of the choroid plexus and its surgical management. *J Neurosurg Pediatr* 5: 518–522, 2010
6) Centeno BA, Louis DN, Kupsky WJ, Preffer FI, Sobel RA: The AgNOR technique, PCNA immunohistochemistry, and DNA ploidy in the evaluation of choroid plexus biopsy specimens. *Am J Clin Pathol* 100: 690–696, 1993
7) D'Ambrosio AL, O'Toole JE, Connolly ES Jr, Feldstein NA: Villous hypertrophy versus choroid plexus papilloma: a case report demonstrating a diagnostic role for the proliferation index. *Pediatr Neurosurg* 39: 91–96, 2003
8) Davis LE: A physio-pathologic study of the choroid plexus with the report of a case of villous hypertrophy. *J Med Res* 44: 521–534.11, 1924
9) Erman T, Gocer AI, Erdogan S, Tuna M, Ildan F, Zorludemir S: Choroid plexus papilloma of bilateral ventricle. *Acta Neurochir (Wien)* 145: 139–143, 2003
10) Fujimoto Y, Matsushita H, Plese JP, Marino R Jr: Hydrocephalus due to diffuse villous hyperplasia of the choroid plexus. Case report and review of the literature. *Pediatr Neurosurg* 40: 32–36, 2004
11) Fujimura M, Onuma T, Kameyama M, Motohashi O, Kon H, Yamamoto K, Ishii K, Tominaga T: Hydrocephalus due to cerebrospinal fluid overproduction by bilateral choroid plexus papillomas. *Childs Nerv Syst* 20: 485–488, 2004
12) Gudeman SK, Sullivan HG, Rosner MJ, Becker DP: Surgical removal of bilateral papillomas of the choroid plexus of the lateral ventricles with resolution of hydrocephalus. Case report. *J Neurosurg* 50: 677–681, 1979
13) Hirano H, Hirahara K, Asakura T, Shimozuru T, Kadota K, Kasamo S, Shimohonji M, Kimotsuki K, Goto M: Hydrocephalus due to villous hypertrophy of the choroid plexus in the lateral ventricles. Case report. *J Neurosurg* 80: 321–323, 1994
14) Iplikcioglu AC, Bek S, Gökduman CA, Bikmaz K, Cosar M: Diffuse villous hyperplasia of choroid plexus. *Acta Neurochir (Wien)* 148: 691–694, 2006
15) Nimjee SM, Powers CJ, McLendon RE, Grant GA, Fuchs HE: Single-stage bilateral choroid plexectomy for choroid plexus papilloma in a patient presenting with high cerebrospinal fluid output. *J Neurosurg Pediatr* 5: 342–345, 2010
16) Philips MF, Shanno G, Duhaime AC: Treatment of villous hypertrophy of the choroid plexus by endoscopic contact coagulation. *Pediatr Neurosurg* 28: 252–256, 1998
17) Shibata Y, Katayama W, Kawamura H, Anno I, Matsumura A: Proton magnetic resonance spectroscopy and 201Thallium-, 99mTechnetium methoxyisobutylisonitrile single photon emission computed tomography findings of a patient with choroid plexus papilloma. *Neuroradiology* 50: 741–742, 2008
18) Smith ZA, Moftakhar P, Malkasian D, Xiong Z, Vinters HV, Lazareff JA: Choroid plexus hyperplasia: surgical treatment and immunohistochemical results. Case report. *J Neurosurg* 107(3 Suppl): 255–262, 2007
19) Tamburrini G, Caldarelli M, Di Rocco F, Massimi L, D'Angelo L, Fasano T, Di Rocco C: The role of endoscopic choroid plexus coagulation in the surgical management of bilateral choroid plexuses hyperplasia. *Childs Nerv Syst* 22: 605–608, 2006
20) Vajtai I, Varga Z, Aguzzi A: MIB-1 immunoreactivity reveals different labelling in low-grade and in malignant epithelial neoplasms of the choroid plexus. *Histopathology* 29: 147–151, 1996
21) Warren DT, Hendson G, Cochrane DD: Bilateral choroid

plexus hyperplasia: a case report and management strategies. *Childs Nerv Syst* 25: 1617–1622, 2009
22) Welch K, Strand R, Bresnan M, Cavazzuti V: Congenital hydrocephalus due to villous hypertrophy of the telencephalic choroid plexuses. Case report. *J Neurosurg* 59: 172–175, 1983

Address reprint requests to: Ryogo Anei, MD, Department of Neurosurgery, Asahikawa Medical College, 2-1 Midorigaoka-Higashi, Asahikawa, Hokkaido 078-8510, Japan.
e-mail: anei@asahikawa-med.ac.jp

Neurol Med Chir (Tokyo) 51, 441～444, 2011

Small Supratentorial, Extraaxial Primitive Neuroectodermal Tumor Causing Large Intracerebral Hematoma

—Case Report—

Jan-Karl BURKHARDT,[1] Ralf A. KOCKRO,[1] Hildegard DOHMEN-SCHEUFLER,[2] Christoph M. WOERNLE,[1] David BELLUT,[3] Spyros KOLLIAS,[3] and Helmut BERTALANFFY[1]

Departments of [1]Neurosurgery, [2]Neuropathology, and [3]Neuroradiology, University Hospital, University of Zurich, Zurich, Switzerland

Abstract

A 16-year-old boy presented with an unusual case of a supratentorial, extraaxial small round blue cell tumor of the central nervous system, which was most likely a primitive neuroectodermal tumor (PNET). Preoperative computed tomography and magnetic resonance imaging showed a large multistage hematoma in the left central region. Intraoperatively, a small, superficial tumorous lesion was found between the sagittal sinus and a large cortical vein hidden by the hematoma. The histological diagnosis was PNET. This tumor is one of the most aggressive intracerebral tumors, not only in children, so treatment strategies must be early, profound, and interdisciplinary. This case represents an important example of atypical extraaxial appearance of this lesion, which should be considered in the differential diagnosis of cortical or subcortical hemorrhage, since complete resection of this lesion is critical for the successful treatment and outcome.

Key words: primitive neuroectodermal tumor, intracerebral hemorrhage, high-grade brain tumor, neurosurgery

Introduction

Supratentorial primitive neuroectodermal tumors (PNETs) belong to a heterogeneous group of undifferentiated or poorly differentiated tumors called small round blue cell tumors (SRBCTs)[9,16] of the central nervous system (CNS), which occur predominantly in children or young adults.[8,12] Recently, supratentorial PNETs were grouped together with all extracerebellar PNETs and renamed CNS PNET.[11] Supratentorial PNETs are less common than cerebellar PNETs and account for 2–3% of all childhood brain tumors with a peak in the first 3 years of life.[18] Preoperative neuroradiological findings vary and may consist of an enhanced lesion on T_1- and T_2-weighted magnetic resonance (MR) imaging or computed tomography (CT) with contrast medium, associated with cystic and necrotic portions, perifocal edema, or hemorrhage.[4] Initiation of early and interdisciplinary adjuvant treatment for PNETs after complete neurosurgical resection is critical for the patient, since these tumors show much more aggressive behavior and the treatment options are poorly defined compared to infratentorial counterparts.

We describe a case of SRBCT obscured by a large intracerebral hemorrhage on preoperative imaging and

Received July 7, 2010; Accepted October 20, 2010

てんかん治療研究振興財団研究年報　2011；22：69-76

慢性硬膜下電極による脳皮質電位計測を用いた側頭葉内側記憶関連野の機能解明

Analysis of memory-related function in medial temporal lobe using electrocorticographic recordings with chronic subdural electrodes

太田貴裕[1)]，鎌田恭輔[2)]，國井尚人[3)]，
川合謙介[3)]，斉藤延人[3)]

要旨：両側側頭葉内側に慢性硬膜下電極を留置した難治性てんかん患者7例で記憶関連課題脳皮質電位（ECoG）計測を行った。記憶機能の優位側決定及び記憶機能特異的な脳皮質活動について加算および時間周波数解析を行った。

加算波形解析では500msec以降の反応が得られ，時間周波数解析ではβ帯域でsynchronization（Syn）続いてdesynchronization（Des）の活動が認められ記憶課題特異的活動と考えられた。High γ帯域では左側で潜時500-800msecのSynが認められた。記憶機能側性化が明らかな5症例ではβ帯域で500-800msecで優位側にSyn，非優位側で800-1000msecにDesを認めた。またhigh γ帯域で優位側に600-800msecでSynの活動が認められた。誘発ECoGを解析することにより記憶優半球同定さらには記憶機能野同定が行える可能性が示された。

てんかん治療研究振興財団研究年報　2011；22：69-76

Key Words：electrocorticography, memory function, event-related potential, time-frequency analysis

序　論

海馬硬化症を伴う薬物治療抵抗性内側側頭葉てんかんに対して選択的海馬扁桃体切除術の有効性が示されているが，頻度は低いものの術後記憶障害が認められること等が現在もなお続く臨床上の問題である。術前の記憶機能を評価することは記憶機能温存目的の手術には必須である。機能MRIや脳磁図をはじめとする脳機能画像の飛躍的な進歩により言語優位半球の同定が可能になってきた。しかし脳磁図では深部磁場の検出が困難なこと，機能MRIでは頭蓋底部の磁化率効果の影響があり，側頭葉内側の脳活動を捉えるのは困難である。これまで記憶の優位機能に関して機能MRIを用いた報告[1, 2)]がなされているが，言語優位半球の同定ほど信頼度が高くないのが現状である。機能MRIは血行動態性の反応を捉えているので時間解像度が低く，記憶課題を行ったとしても想起の結果としてのプロセスを捉えているのか，違った情報の想起を直接反省するプロセスを示しているのかはっきり分けることができない。

現時点で術前に記憶優位半球を同定する方法は Wada testのみである[3)]。しかし海馬の血流

[1)] 東京都立多摩総合医療センター　脳神経外科，[2)] 旭川医科大学　脳神経外科
[3)] 東京大学医学部　脳神経外科
[1)] Department of Neurosurgery, Tokyo Metropolitan Tama Medical Center
2-8-29, Musasi-dai, Fuchu, Tokyo, 183-8524, Japan
[2)] Department of Neurosurgery, Asahikawa Medical University
[3)] Department of Neurosurgery, The University of Tokyo

支配は後大脳動脈の分枝である海馬動脈であり，内頚動脈より静脈麻酔薬を注入するWada testで海馬の機能抑制が十分に行われているかどうか疑問もあり，術後の言語性記憶の結果を予測することに限界があるという報告がある[4]。記憶機能温存には，記憶機能野の同定と解剖学的局在の詳細な把握と，それを可能にする術前評価方法の確立が必要である。

内側側頭葉は叙述記憶プロセス（事実，出来事）に必須の役割を果たしている[5]。認識記憶，つまり以前に刺激提示があったものかを判断する能力は内側側頭葉によって補助される叙述記憶の1タイプであり，病巣研究[6]，電気生理学研究[7]，機能MRIにより内側側頭葉周辺が関与している証拠が示されている。一方，海馬を中心とした側頭葉内側の活動を捉える電気生理学的手法として深部電極[8]あるいは硬膜下電極[9) 15)]を用いたECoG計測の方法が報告されている。事象誘発脳波の評価方法としてevent-related synchronization/desynchronization: ERS/ERDがあり，記憶や言語など時間経過でダイナミックに変化する認知機能の研究には時間分解能が優れているため適している[9]。これまでの脳機能画像研究から推察されることは，異なった脳の箇所で多くの神経集合体が記憶の形成および後に続く想起に関与しているということである。そのようなネットワークは広範なまた機能的に異なった皮質領域の神経活動のERSによって構築されている[10]。猿において視覚性認識記憶課題を行い海馬での神経活動を計測したところγ帯域のERSの増加が計測されたことにより，海馬ニューロン間で協調が増強されたことを反映していると結論している[11]。ヒトにおいては25Hz以上のγ帯域反応がこのようなネットワークや細胞集合体の活動を示すものとして議論されてきており[12, 13]，working memoryにgamma oscillationが関係していると報告されている[14), 15)]。

現在脳機能局在法のgold standardは皮質電気刺激マッピング法である。しかし記憶機能に主に関与する側頭葉内側部の電気刺激は，てんかん焦点に近く発作を誘発する可能性が高いこと，三叉神経の刺激により痛みを伴うことが多いことなどから長時間，広範囲にわたり行うことは現実的には困難である。これまでの脳機能画像とは異なり，慢性硬膜下電極は脳表から直接脳皮質電位（electrocorticography：ECoG）を計測することができるため深部である側頭葉内側面からの誘発電位を計測することが可能である。慢性硬膜下電極による頭蓋内脳波計測は侵襲的でありその対象が限局されつつあるが，焦点が両側性あるいは広範囲にわたる場合には留置は必須である。そこで我々は電気刺激マッピングに代わる方法として，慢性硬膜下電極を用いた誘発皮質電位計測を取り入れてきた。

本研究では記憶課題を用いて慢性硬膜下電極による誘発ECoGの計測・データ解析を行った。記憶機能の優位側決定が可能かどうか，また記憶機能に特異的な側頭葉内側の脳活動について加算波形および時間周波数解析(Wavelet解析)での検討を行った。

2．対象と方法

（1）対象

東京大学医学部付属病院において2006年から2008年にかけて難治性てんかん患者にてんかん焦点同定のために慢性硬膜下電極を留置した症例のうち，側頭葉内側に両側対称性に慢性硬膜下電極を留置した7例を対象とした（Tab. 1）。全例Wada testを施行し言語優位半球，記憶優位半球（言語性，視覚性）を同定した。また術前にWAIS-R, WMS-Rを全例に施行し高次機能評価を行った。

（2）電極留置

てんかんの焦点精査目的に両側側頭葉底面，前頭葉外側面，側頭葉外側面などに硬膜下電極を留置した。側頭葉内側（鉤から海馬傍回にかけて）に留置した8極電極（Fig. 1A）については術中に透視で位置を確認した。術後はMRIから脳表3D画像を作成しCTから得られた電極位置とレジストレーションし合成画像を作成することで電極位置を確認した。各症例の側頭葉底面での電極位置をFig. 2に示した。海馬を中心とした内側側頭葉での活動を解析対象とするため，図で示した左右で計16極のみを解析対象とした。

Tab. 1　Clinical characteristics for 7 patients

	Age/Sex	Focus	verbal memory	visual memory	WMS-R（言語）	WMS-R遅延
Case 1	35F	Lt temporal,	Lt	Lt	116	117
Case 2	33F	Lt orbitofrontal Lt lateral temporalp	Bil	Lt	111	118
Case 3	24M	Lt temporal	Lt	Lt	-2SD	-2SD
Case 4	40M	Rt temporal	Rt	Rt	118	99
Case 5	49F	Rt temporal	Lt	Rt	112	111
Case 6	20M	Lt temporal	Lt	Bil	99	108
Case 7	36F	Lt temporal	Rt	Rt	109	77

M: male, F: female, Rt: right, Lt: left, Bil: bilateral

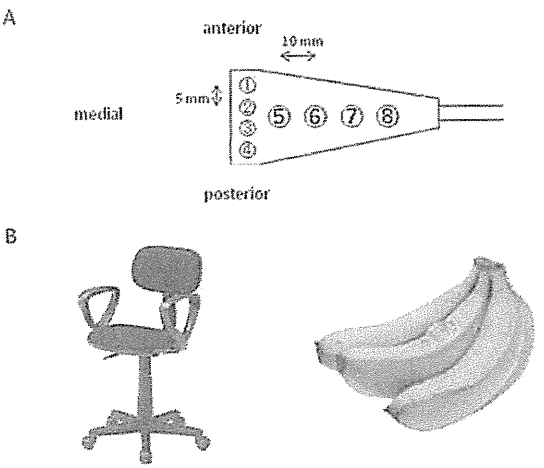

Fig. 1　A) The subdural electrode placed on the left temporal base
B) Examples of memory-task figures

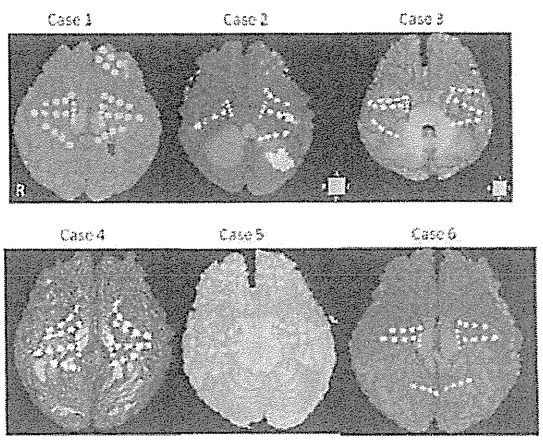

Fig. 2　The location of the subdural electrodes on both the temporal bases (cases 1–6) The electrodes were registered by 3D-magnetic resonance imaging (MRI) in each patient. On the temporal base, the grids were placed almost symmetrically.

(3) 慢性硬膜下電極による誘発ECoGの計測

ECoG記録にはBMSI6000 (Nicolet Biomedical Inc. Wisconsin) 脳波計 (128ch) を用い，通常の脳波条件下 (0.55-150Hzのアナログフィルター) で記録を行った。

①物品呼称（絵を見せて名前を考えてもらう：Pic)，②P300課題 (1Hz, 500kHzの音を聞かせる，500Hzをrare stimulusとし20％)，③記憶課題（あらかじめ検査前に10個の絵を覚えてもらう (Fig. 1B)，約10分後物品呼称で用いたのと同じ絵を用いて記憶対象群の絵が提示されたときにボタンを押す：Memory）を行い，認知ECoGを取得した。記憶課題は物品呼称課題で使用した絵をあらかじめ覚えさせておき提示した絵が既視かどうかを判断させボタン押しで回答させた。ECoGはサンプリング周波数400Hzで海馬を含む脳全体のECoGを同時に計測した。

(4) 電位の解析

データ解析はEMSE (Source Signal Imaging, Inc. San Diego, USA) を用いた。

解析区間は刺激提示から1000msecとした。加算と周波数解析ではデジタルフィルターはかけていない。ECoG生データは時間-周波数解析 (Wavelet解析) を行い，脳皮質領域毎の経時的

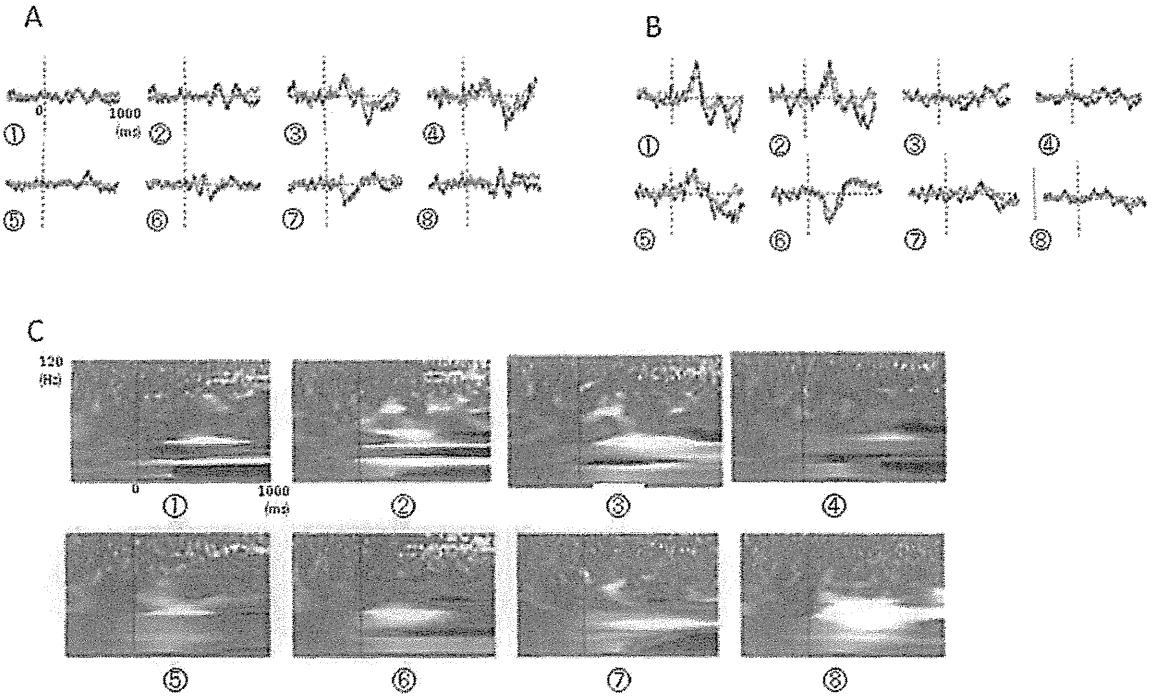

Fig. 3 Results of the averaging analysis (−500 ms～1000 ms) of the memory task (black line) in case 2. The electrodes on the right temporal base showed major positive peak around 500–600ms in channels (chs) ③ and ④ (A). On the left side, a major negative peak around 500 ms appeared in chs ① and ② (B). (C) The results of the wavelet analysis on the left temporal base showed synchronization around 500–800ms in the β and γ bands and around 500–1000 ms in the high γ band.

変化の解析を行った。加算波形（100回加算）振幅の解析により有意波形の検出，記憶特異的反応を検出するために記憶課題波形－物品呼称波形のoverlayを行った。

波形同期の解析に時間—周波数（Wavelet）解析にて，周波数成分をβ（20-35Hz），γ（35-80Hz），high γ（80-120Hz）bandの3つに区分し，100msecごとの活動（ERS/ERD）を比較し，どの周波数帯域で，どの時間帯が有意所見となるのかの検討をすすめた。

3．結　　果

（1）加算波形（Fig. 3）

記憶課題と物品呼称課題との比較

左内側側頭葉切除後であるCase 7を除いた6例で解析を行った。内側側頭葉（ch1-6）では右側で500-700msecでpositive peak 3例，600-700msecでnegative peak 2例に認められた。左側では500-600msecでのpositive peakが1例，800msec前後にnegative peakが3例，700-800msec付近でのpositive peakが2例に認められた。外側のch7-8では1例のみで500msec付近にpositive peakを認めた。

つまり刺激提示後500msec以降で positive peakが見られたのが右側4例，左側4例，またnegative peakが見られたのは右側2例，左側3例でありこれらの反応は記憶課題特異的波形と考えられたが，明らかな左右差は認められなかった。2例（Case 3, 4）では明らかな記憶課題特異的な波形が検出できなかった。Case 3は高次機能障害を認めておりCase 4もWMS-R（遅延再生）が99と6人の中で最低であった。

P300課題では右側で波形が検出できたのがch2-3で4例，左では3例であり，3例で有意な波形を認められなかった。透視下での電極留置は海馬傍回に対して個人で位置が異なってくるた

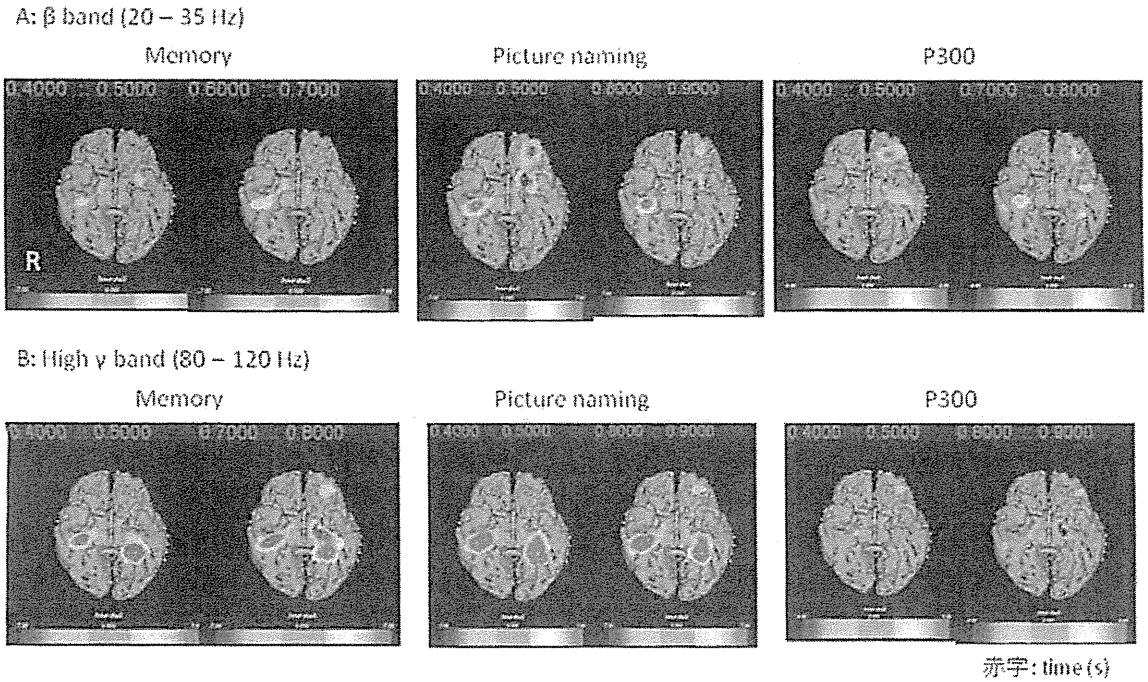

Fig. 4　The figure shows the results of the wavelet analysis on the temporal base in the β band (A) and high γ band (B) in case 2.
Red area indicates "synchronization" and blue area indicates "desynchronization." In the β band, synchronization appeared in both the medial temporal lobes (Memory) and in the right temporal base (Picture naming), whereas there was desynchronization in the left medial temporal lobe (P300). In the high γ band, strong synchronization appeared in both the medial temporal lobes (Memory, Picture naming) whereas there was desynchronization in the left medial temporal lobe (P300).

Tab. 2　各周波数帯域での時間（msec）ごとのsynchronization（ERS）とdesynchronization（ERD）のパターン

	Memory		Pic		P300	
	Lt	Rt	Lt	Rt	Lt	Rt
β band	500-800 ERS 4 800-1000 ERD 5	500-800 ERS 5 800-1000 ERD 4	400-500 ERD 3 700-1000 ERS 4	300-500 ERD 5 700-1000 ERS 5	300-500 ERS 4 300-500 ERD 4	400-500 ERS 3 300-400 ERD 3 500-600 ERD 3
γ band	500-800 ERS 1 ERD 1	500-800 ERS 3	800-1000 ERS 1	600-800 ERS 4	300-500 ERS 3	300-500 ERS 2
high γ band	500-800 ERS 3 ERD 1	600-900 ERS 6 ERD 0	300-400 ERS 2 500-800 ERS 2 800-1000 ERS 3	400-600 ERS 5 600-1000 ERS 7	300-500 ERS 3	400-600 ERS 5

め加算波形だけでの評価は困難と考えられた。

（2）時間周波数解析（Fig. 4, Tab. 2）

PicとMemoryの比較であるが，β帯域では左側で500-800msecでERSを，800-1000msecでERDが5例に認められた。対してPicではERD，ERSの順であった。γ帯域では両課題とも左ではほとんど活動が認められなかった。右側で600-800msecにおいてERSを認め記憶特異的ではなく視覚情報入力によるものと考えられた。High γ

帯域ではどちらの課題でも左側で潜時500-800 msecのERSが認められた。

P300課題ではβ帯域において300-500msecでのERS 4例，ERD3例に認めγ，high γ帯域ともにERDは認められなかった。

（3）視覚性記憶優位半球の検討

Wada testで側性化が明らかな（Case1-5）5症例で，記憶機能の優位側と非優位側でのWavelet解析の結果を比較した。β帯域で潜時500-800msecで優位側にERS，非優位側で潜時800-1000msecにERDを認めた例が3症例あった。γ帯域では活動がほとんど捉えられなかった。またhigh γ帯域で優位側に潜時600-800msecでERSの活動が認められた症例が2例認められた。これらの結果により記憶課題でWavelet解析を行うことで記憶優位半球の同定の可能性が高まった。

（4）左海馬切除後であるCase 7での検討

Case 7はWMS-R遅延再生が77と低値を認めており課題遂行が困難であった。加算波形ではどの課題でも有意波形を捉えられていない。右内側側頭葉のWavelet解析では，β帯域，γ帯域ではっきりした活動はみられず，high γ帯域でMemory，Picとも600-1000msecでERS，P300では400-600msecでのERSを認めた。

4. 考　　察

P300に関連するevent-related gamma band oscillationが440.5msから始まり約100ms持続するという報告[16]や，ERPの研究では内側側頭葉前部でのN400，海馬でのP600が認識記憶に関連しているとされている[8]。本研究での加算波形の結果からは刺激提示後500msec以降でpositive peakが見られたのが左右4例ずつ，またnegative peakが見られたのは右2例，左3例であり記憶課題特異的波形と考えられた。一方WMS-Rが低い2症例では有意な波形が計測できておらず，課題がこなせないと加算結果が得られない可能性や，電極位置がかならずしも海馬周辺に精度高く留置できるわけではないことが加算波形の結果が安定しない理由として考えられる。電極位置の正確性に関しては深部電極が勝ると考えられる。

頭蓋内電極θとγ（28-64Hz）oscillatory activityが新規叙述記の形成に関与しているという報告[17]がある。本研究での時間周波数解析ではβ帯域において500-800msのERS，その後のERDの活動が記憶機能特異的である可能性がある。high γ帯域においては左で500-800msのERSがMemory，Picとも認められた。一方右側では600ms以降のERSについてPicの方が割合が高かった。

Wada testのみが記憶優位半球を同定できる方法であり各種画像検査の限界が認められている現在，本研究で示された記憶課題により視覚性優位半球を術前に評価できる可能性が示されたことは今後の臨床応用につながるものと考えられる。内側側頭葉てんかん患者においてfMRIによるmemory encodingのlateralizationがWada testと9人中8人で一致していたという報告がある[1]。β帯域において500-800msではっきりしたERSを認め，対側で800-1000msでERDを認める場合には，ERSを示す側が優位の可能性がある。またhigh γ帯域では600-800msでERSを認め対側に見られない場合にはそちらが優位半球の可能性がある。今後症例数を積み重ねてさらに精度を高めることにより，記憶機能温存を意図した側頭葉内側切除に際しての方針決定因子となりうると考えられる。

今回の硬膜下電極は厳密には海馬というより海馬傍回皮質上に留置してある。認知機能は内側側頭葉内で複数の信号が関わる動的プロセスであり，novelty, recenty, familiarityを認知し，海馬傍回に認知記憶を支持する構造があることが推測されている[18]。また海馬が想起に最も関与しており，単純な親密さの部位認知にはあまり関与していない可能性や，海馬は過去の経験つまり想起，親密さを認知する部位であると報告されている[19]。本研究ではWada testで使用している視覚記憶課題を用いており，この課題は想起を利用して海馬機能を評価しているものと考えられているものである。しかし内側側頭葉内の詳細な機能分布の検討のためにはさらに留置部位の厳密性，電極サイズの縮小化，複数

の課題の応用などが必要と考えられる。

皮質電気刺激は最も確立したマッピング法であるが内側側頭葉はてんかん焦点に近く，痛みも伴うことが多いことから詳細な検討が難しい。本研究で示したように誘発ECoG計測を解析することにより記憶優半球同定さらには記憶機能野同定が行える可能性が示され，今後てんかん術前評価目的の新たなマッピング法として有用であると考えられた。

5．文　献

1) Golby AJ, Poldrack RA, Illes J, Chen D, Desmond JE, Gabrieli JD. Memory lateralization in medial temporal lobe epilepsy assessed by functional MRI. Epilepsia 2002；43：855-863.

2) Ramsoy TZ, Liptrot MG, Skimminge A, Lund TE, Sidaros K, Christensen MS, et al. Regional activation of the human medial temporal lobe during intentional encoding of objects and positions. Neuroimage 2009；47：1863-1872.

3) Paglioli E, Palmini A, Portuguez M, Paglioli E, Azambuja N, da Costa JC, et al. Seizure and memory outcome following temporal lobe surgery: selective compared with nonselective approaches for hippocampal sclerosis. J Neurosurg 2006；104：70-78.

4) Kirsch HE, Walker JA, Winstanley FS, Hendrickson R, Wong ST, Barbaro NM, et al. Limitations of Wada memory asymmetry as a predictor of outcomes after temporal lobectomy. Neurology 2005；65：676-680.

5) Milner B, Squire LR, Kandel ER. Cognitive neuroscience and the study of memory. Neuron 1998；20：445-468.

6) Suzuki WA, Zola-Morgan S, Squire LR, Amaral DG. Lesions of the perirhinal and parahippocampal cortices in the monkey produce long-lasting memory impairment in the visual and tactual modalities. J Neurosci 1993；13：2430-2451.

7) Xiang JZ, Brown MW. Differential neuronal encoding of novelty, familiarity and recency in regions of the anterior temporal lobe. Neuropharmacology 1998；37：657-676.

8) Klaver P, Fell J, Dietl T, Schur S, Schaller C, Elger CE, et al. Word imageability affects the hippocampus in recognition memory. Hippocampus 2005；15：704-712.

9) Karrasch M, Laine M, Rapinoja P, Krause CM. Effects of normal aging on event-related desynchronization/synchronization during a memory task in humans. Neurosci Lett 2004；366：18-23.

10) Singer W, Gray CM. Visual feature integration and the temporal correlation hypothesis. Annu Rev Neurosci 1995；18：555-586.

11) Jutras MJ, Fries P, Buffalo EA. Gamma-band synchronization in the macaque hippocampus and memory formation. J Neurosci 2009；29：12521-12531.

12) Keil A, Gruber T, Muller MM. Functional correlates of macroscopic high-frequency brain activity in the human visual system. Neurosci Biobehav Rev 2001；25：527-534.

13) Tallon-Baudry C, Bertrand O. Oscillatory gamma activity in humans and its role in object representation. Trends Cogn Sci 1999；3：151-162.

14) Howard MW, Rizzuto DS, Caplan JB, Madsen JR, Lisman J, Aschenbrenner-Scheibe R, et al. Gamma oscillations correlate with working memory load in humans. Cereb Cortex 2003；13：1369-1374.

15) Mainy N, Kahane P, Minotti L, Hoffmann D, Bertrand O, Lachaux JP. Neural correlates of consolidation in working memory. Hum Brain Mapp 2007；28：183-193.

16) Watanabe N, Hirai N, Maehara T, Kawai K, Shimizu H, Miwakeichi F, et al. The relationship between the visually evoked P300 event-related potential and gamma band oscillation in the human medial and basal temporal lobes: an electrocorticographic study. Neurosci Res 2002；44：421-427.

17) Sederberg PB, Kahana MJ, Howard MW, Donner EJ, Madsen JR. Theta and gamma